Complex Scaled Tangent Rotations (CSTAR) for Fast Space–Time Adaptive Equalization of Wireless TDMA

Massimiliano (Max) Martone, *Member, IEEE*

***Abstract*—A new update algorithm for space–time equalization of wireless time-division multiple access signals is presented. The method is based on a modified QR factorization that reduces the computational complexity of the traditional QR-decomposition based recursive least squares method and maintains numerical stability. Square roots operations are avoided due to the use of an approximately orthogonal transformation, defined complex scaled tangent rotation.**

***Index Terms*—Adaptive equalizers, decision feedback equalizers, land–mobile radio cellular systems.**

I. Introduction

THE SPACE–TIME equalization concept was first proposed in [1] and subsequently applied to wireless time-division multiple access (TDMA) in [2] where it was conjectured the implicit optimality of the scheme. The use of different feed forward filters at the antennas and one single feedback filter was demonstrated to be effective because it was able to simultaneously combat signal fading, intersymbol and cochannel interference. The implementation of the joint update requires special attention because low signal-to-noise ratio and fast frequency selective fading channels result generally in ill-conditioned adaption. Recursive least squares based on QR decomposition [3] is a well-known and numerically well-behaved method to perform the filters update. However, the high computational complexity of the method has always been considered a remarkable problem. We propose in this work a new algorithm based on an approximated QR factorization which improves in terms of computational efficiency over existing schemes mainly because square roots operations are avoided. The approach uses a generalization of the scaled tangent rotation of [5] to update the Cholesky factor of the information matrix without needing to form it. The performance of the method is compared to more traditional algorithms by means of computer simulations in fixed point arithmetic for a realistic scenario, as specified in the standard IS-136 [6], [7] for cellular communications in the U.S.

II. Space–Time QR-Based MMSE Equalization

Consider a two-antenna receiver.[1] At the kth antenna P_k delayed and attenuated replicas of the signal are received ($k = 1, 2$). The impulse response of the two multipath diversity channels can be expressed as $f_k(t) = \sum_{m=1}^{P_k} \rho_{m,k} e^{j\psi_{m,k}} \delta(t - \tau_{m,k})$, $k = 1, 2$ where $\tau_{m,k}$, $\rho_{m,k}$, and $\psi_{m,k}$ are the delay, amplitude, and phase of the mth path, respectively, as received at the kth antenna. The complex baseband modulated signal is $m(t) = \sum_m x_m \; p_g(t - mT)$, where $x_m = a_m + j \; b_m$ are the complex symbols defining the signal constellation used for the particular digital modulation scheme.[2] The filter $p_g(t)$ is a square root raised cosine shaping filter with rolloff factor equal to 0.35 and T is the signaling interval. The baseband signal received at the kth antenna is $r_k(t) = \sum_{m=1}^{P_k} \rho_{m,k} m(t - \tau_{m,k}) e^{j\phi_{m,k}} + \tilde{n}_k(t)$ where $\phi_{m,k} = -2\pi f_0 \tau_{m,k} + \psi_{m,k}$, f_0 is the carrier frequency, and $\tilde{n}_k(t)$ is additive Gaussian noise. $r_k(t)$ is sampled at R/T rate (R is an integer usually in the range $1, \cdots, 8$) and square root raised cosine filtered to obtain the complex I/Q fractionally spaced samples $y_n^{(k)}$, $k = 1, 2$. The optimum combining/equalization scheme has two feedforward filtering sections (one per antenna) and one feedback filtering section (see Fig. 1). Since the algorithm jointly optimizes the taps of these filters as to minimize the mean squared error using samples of the received signal taken at different points in time and in space, this architecture is called space–time minimum mean-square error (MMSE) equalizer. We can express the output of the MMSE space–time equalizer in vector notation as

$$z_n = \mathbf{y}(n)^T \mathbf{c}(n)$$

where[3]

$$\begin{aligned}
\mathbf{y}(n) &= [\mathbf{y}_{f_1}(n)^T, \mathbf{y}_{f_2}(n)^T, \mathbf{y}_b(n)^T]^T \\
\mathbf{c}(n) &= [\mathbf{c}_{f_1}(n)^T, \mathbf{c}_{f_2}(n)^T, \mathbf{c}_b(n)^T]^T \\
\mathbf{c}_{f_1}(n) &= [c_{-L_1}^{(1)_f}(n), c_{-L_1+1}^{(1)_f}(n), \cdots, c_0^{(1)_f}(n)]^T \\
\mathbf{c}_{f_2}(n) &= [c_{-L_1}^{(2)_f}(n), c_{-L_1+1}^{(2)_f}(n), \cdots, c_0^{(2)_f}(n)]^T \\
\mathbf{y}_{f_1}(n) &= [y_{n+L_1}^{(1)}, y_{n+L_1-1}^{(1)}, \cdots, y_n^{(1)}]^T \\
\mathbf{y}_{f_2}(n) &= [y_{n+L_1}^{(2)}, y_{n+L_1-1}^{(2)}, \cdots, y_n^{(2)}]^T \\
\mathbf{y}_b(n) &= [x_{n-1}, x_{n-2}, \cdots, x_{n-L_2}]^T \\
\mathbf{c}_b(n) &= [c_1^b(n), c_2^b(n), \cdots, c_{L_2}^b(n)]^T.
\end{aligned}$$

The adaptive algorithm minimizes the mean-squared error defined as $\mathrm{MSE} = E\{|\epsilon_n|^2\} = E\{|x_n - z_n|^2\}$, and the goal of the adaption process is to adjust $\mathbf{c}(n)$ (size $L = L_2 + 2(L_1 + 1)$) to converge toward the solution $\mathbf{c}_{opt} = E\{\mathbf{y}(n)\mathbf{y}(n)^H\}^{-1} E\{\mathbf{y}(n)^* x_n\}$. The sequence x_n is generated using the known

Paper approved by S. B. Gelfand, the Editor for Transmission Systems of the IEEE Communications Society. Manuscript received April 7, 1997; revised December 3, 1997. This paper was presented at the Eighth Virginia Tech Symposium on Wireless Personal Communications, Blacksburg, VA, June 1998.

The author is with the Watkins-Johnson Company, Telecommunications Group, Gaithersburg, MD 20878-1794 USA (e-mail: max.martone@wj.com).

Publisher Item Identifier S 0090-6778(98)09392-1.

[1] We treat here the two-antenna case because it is of high practical interest although no particular problem is in the generalization of the method to more than two antennas.

[2] This is $\pi/4$ DQPSK in the U.S. standard for cellular communications [6].

[3] Note that $\mathbf{c}_l^{(k)_f}(n)$, $k = 1, 2$ are fractionally spaced taps, while $\mathbf{c}_l^b(n)$ are symbol spaced taps. Moreover, $\mathbf{c}(n)$ is updated once per symbol.

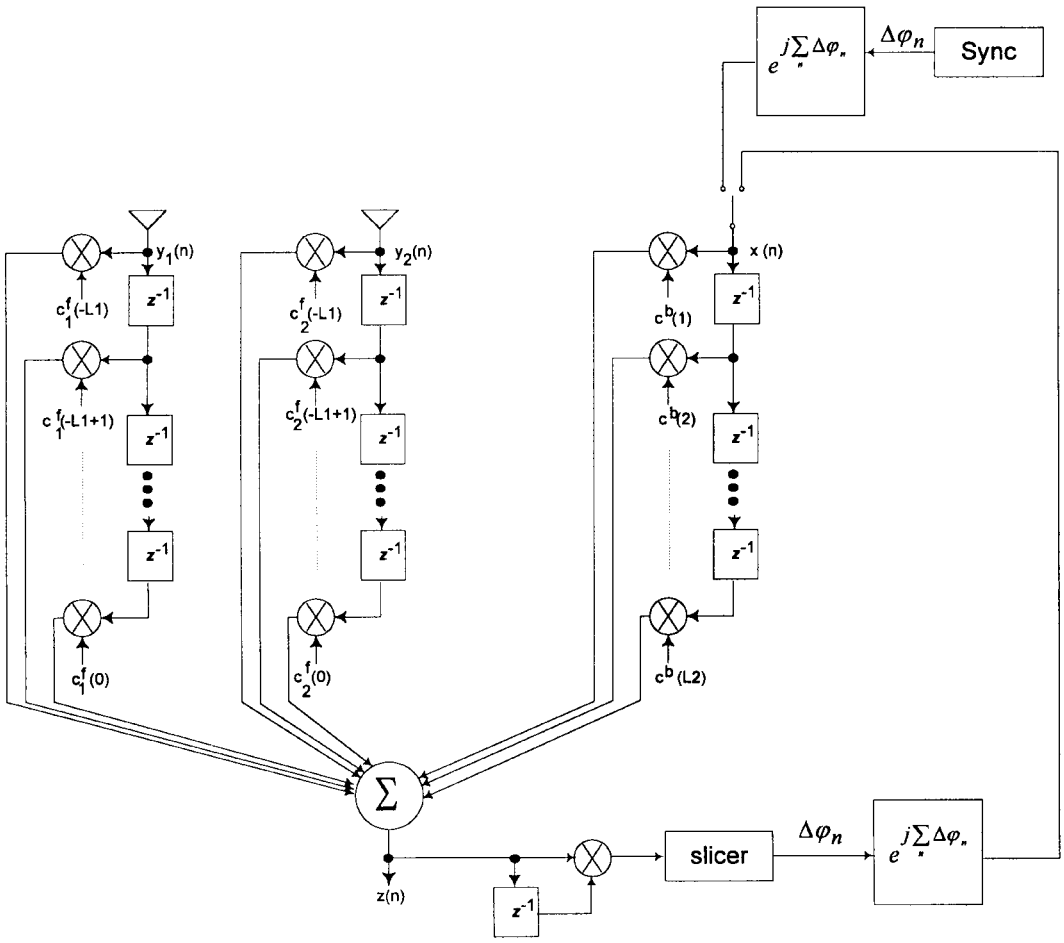

Fig. 1. The space–time MMSE equalizer architecture.

training symbols (during training) and using past decisions (during data demodulation, in decision directed mode).

The QR Approach: The equalization problem can be reconducted to solving at each $n+1$ step the problem

$$\min_{\mathbf{c}} \left\| \begin{bmatrix} \lambda \tilde{\mathbf{Y}}^{(n)} \\ \mathbf{y}(n+1)^T \end{bmatrix} \mathbf{c} - \begin{bmatrix} \lambda \mathbf{X}^{(n)} \\ x_{n+1} \end{bmatrix} \right\|^2 \tag{1}$$

where λ is the *forgetting factor* [3], $\tilde{\mathbf{Y}}^{(n)^T} = [\mathbf{y}(1), \mathbf{y}(2), \cdots, \mathbf{y}(n)]\mathbf{\Lambda}(n)$ is the data matrix, and $\mathbf{X}^{(n)^T} = [x_1, x_2, \cdots, x_n]\mathbf{\Lambda}(n)$ with $\mathbf{\Lambda}(n) = \mathrm{diag}[\lambda^{n-1}, \lambda^{n-2}, \cdots, 1]$. The *normal equations* define the desired minimizer as $\tilde{\mathbf{Y}}^{(n+1)^H}\tilde{\mathbf{Y}}^{(n+1)}\mathbf{c} = \tilde{\mathbf{Y}}^{(n+1)^H}\mathbf{X}^{(n+1)}$. The use of orthogonal transformation to solve least squares problems is well established as is the inadvisability of using the normal equations [3]. Suppose that a matrix $\mathbf{V}^{(n)}$ is known from the previous step such that $\mathbf{Q}\tilde{\mathbf{Y}}^{(n)} = \begin{bmatrix} \mathbf{V}^{(n)} \\ \mathbf{0} \end{bmatrix}$, with $\mathbf{Q}$ orthogonal and $\mathbf{V}^{(n)}$ upper triangular matrix, then the problem stated in (1) is equivalent to

$$\min_{\mathbf{c}(n+1)} \left\| \begin{bmatrix} \lambda \mathbf{V}^{(n)} \\ \mathbf{y}(n+1)^T \end{bmatrix} \mathbf{c}(n+1) - \begin{bmatrix} \lambda \hat{\mathbf{X}}^{(n)} \\ x_{n+1} \end{bmatrix} \right\|^2 \tag{2}$$

where

$$\mathbf{Q}\mathbf{X}^{(n)} = \begin{bmatrix} \hat{\mathbf{X}}^{(n)} \\ r \end{bmatrix}$$

because Euclidean distance is preserved by orthogonal transformations. The traditional QR-RLS approach [3] obtains $\mathbf{c}(n+1)$ from the solution of the triangular linear system $\mathbf{V}^{(n+1)}\mathbf{c}(n+1) = \hat{\mathbf{X}}^{(n+1)}$ where $\mathbf{V}^{(n+1)}$ is obtained by sweeping the row vector $\mathbf{y}(n+1)^T$ in (2) through orthogonal transformations represented by $\tilde{\mathbf{Q}}(n)$ and $\hat{\mathbf{X}}^{(n+1)}$ is obtained applying the same orthogonal transformations to $[\lambda \hat{\mathbf{X}}^{(n)^T}, x_{n+1}]^T$.

III. CSTAR Transformation and the New Method

The novelty of the method we present is in the following two points.

1) The algorithm tracks the variation in $\mathbf{c}(n)$ from step n to step $n+1$ rather than $\mathbf{c}(n)$ itself. This saves multiplications.
2) The orthogonal transformations are approximated by scaled tangent rotations rather than the traditional Givens rotations. This avoids the need for square root operations.

Define $\partial\mathbf{c}(n) = \mathbf{c}(n+1) - \mathbf{c}(n)$. From the previous section $\tilde{\mathbf{Q}}(n)$ is such that

$$\tilde{\mathbf{Q}}(n)\begin{bmatrix} \lambda \mathbf{V}^{(n)} \\ \mathbf{y}(n+1)^T \end{bmatrix} = \begin{bmatrix} \mathbf{V}^{(n+1)} \\ \mathbf{0}^T \end{bmatrix}$$

with $\mathbf{V}^{(n+1)}$ upper triangular. Since

$$\tilde{\mathbf{Q}}(n)\left\{\begin{bmatrix}\lambda\hat{\mathbf{X}}^{(n)}\\ x_{n+1}\end{bmatrix}-\begin{bmatrix}\lambda\mathbf{V}^{(n)}\\ \mathbf{y}(n+1)^T\end{bmatrix}\mathbf{c}(n)\right\}=\tilde{\mathbf{Q}}(n)\begin{bmatrix}\mathbf{0}\\ u_{n+1}\end{bmatrix} \tag{3}$$

$\partial\mathbf{c}(n)$ is the solution of[4]

$$\min_{\partial\mathbf{c}(n)}\left\|\begin{bmatrix}\mathbf{V}^{(n+1)}\\ \mathbf{0}^T\end{bmatrix}\partial\mathbf{c}(n)-\tilde{\mathbf{Q}}(n)\begin{bmatrix}\mathbf{0}\\ u_{n+1}\end{bmatrix}\right\|^2 \tag{4}$$

where $u_{n+1}=x_{n+1}-\mathbf{y}(n+1)^T\mathbf{c}(n)$. Hence $\partial\mathbf{c}(n)$ can be found by solving the triangular system

$$\mathbf{V}^{(n+1)}\,\partial\mathbf{c}(n)=\overline{\mathbf{X}}^{(n+1)} \tag{5}$$

where $\overline{\mathbf{X}}^{(n+1)}$ satisfies

$$\begin{bmatrix}\overline{\mathbf{X}}^{(n+1)}\\ r_{n+1}\end{bmatrix}=\tilde{\mathbf{Q}}(n)\begin{bmatrix}\mathbf{0}\\ u_{n+1}\end{bmatrix}.$$

It is then evident that all we need to solve the system (5) can be obtained by forming

$$\tilde{\mathbf{V}}^{(n)}=\begin{bmatrix}\lambda\mathbf{V}^{(n)} & \mathbf{0}\\ \mathbf{y}(n+1)^T & u_{n+1}\end{bmatrix}$$

and sweeping the bottom part of this matrix using plane rotations.[5] The orthogonal matrix $\tilde{\mathbf{Q}}(n)$ can be found as a product of$L=L_2+2(L_1+1)$ Givens rotation matrices [3]: $\tilde{\mathbf{Q}}(n)=\tilde{\mathbf{Q}}(n)^{(1)}\tilde{\mathbf{Q}}(n)^{(2)}\cdots\tilde{\mathbf{Q}}(n)^{(L)}$. A single Givens rotation $\tilde{\mathbf{Q}}(n)^{(l)}$ annihilates the $L+1$, l-element $\tilde{v}^{(n)}_{L+1,\,l}$ ($l=1,2,\cdots,L$) of $\tilde{\mathbf{V}}^{(n)}$ using $\tilde{v}^{(n)}_{l,\,l}$: $\tilde{\mathbf{Q}}(n)^{(l)}_{k,\,k}=1\ k\neq l,\ L+1$, $\tilde{\mathbf{Q}}(n)^{(l)}_{k,\,m}=0$, $\tilde{\mathbf{Q}}(n)^{(l)}_{L+1,\,L+1}=c_l$, $\tilde{\mathbf{Q}}(n)^{(l)}_{l,\,L+1}=s_l$, $\tilde{\mathbf{Q}}(n)^{(l)}_{L+1,\,l}=-s_l^*$, $\tilde{\mathbf{Q}}(n)^{(l)}_{l,\,l}=c_l$, where

$$c_l=|\tilde{v}^{(n)}_{l,\,l}|/\sqrt{|\tilde{v}^{(n)}_{l,\,l}|^2+|\tilde{v}^{(n)}_{L+1,\,l}|^2}$$

and

$$s_l=\tilde{v}^{(n)*}_{L+1,\,l}/\sqrt{|\tilde{v}^{(n)}_{l,\,l}|^2+|\tilde{v}^{(n)}_{L+1,\,l}|^2}(\tilde{v}^{(n)}_{l,\,l}/|\tilde{v}^{(n)}_{l,\,l}|).$$

The considerable drawback of the method is in the computation of the angles for the Givens rotations. Square-root computations are not easily implemented in DSP processors and are even more problematic in VLSI circuits. Usually they involve iterative procedures whose convergence is not always guaranteed. Scaled tangent rotations (STAR) were proposed in the context of RLS adaptive filtering for real time-series in [5]. We generalize the rotation to the complex domain but there is a difference that is important to note. In STAR [5] scaling is necessary to prevent instability caused by the fact that the tangent function may become infinite. Our modification for complex signals still contains a scaling operation but the factors *are not normalized to unity* as in [5] because this would involve again a square-root operation. The CSTAR (complex scaled tangent rotation) transformation $\mathbf{T}(n)=\mathbf{T}(n)^{(1)}\mathbf{T}(n)^{(2)}\cdots\mathbf{T}(n)^{(L)}$ in analogy to the Givens rotation is defined in terms of each $\mathbf{T}(n)^{(l)}$ as in Table I, where the complex sign function is $c\text{sign}\{x\}=(1/\sqrt{2})\text{sign}\{\text{Real}[x]\}+(j1/\sqrt{2}\text{sign}\{\text{Imag}[x]\})$ and the sweep is applied to the augmented matrix $\tilde{\mathbf{V}}^{(n)}$ (see Table II). Observe that the Givens elementary complex rotation has two remarkable properties. First of all it zeros selectively one predetermined element of any complex matrix, which is indeed needed to triangularize the data matrix. Second, it is an orthogonal transformation, that is $\tilde{\mathbf{Q}}(n)^{(l)}$ is an orthogonal matrix that preserves the original least squares problem. The CSTAR elementary transformation $\mathbf{T}(n)^{(l)}$ maintains the first property but it is not an orthogonal transformation. Note

[4]Just substitute $\mathbf{c}(n+1)=\mathbf{c}(n)+\partial\mathbf{c}(n)$ in (2) and use (3).

[5]It should be clear now that by tracking $\partial\mathbf{c}(n)$ we have simplified the rotation step in $\mathbf{V}^{(n)}$ because the first L elements of the last column of $\tilde{\mathbf{V}}^{(n)}$ are equal to zero. We save $2L$ complex multiplications with respect to the QR-RLS of [3] and, more important, the dynamic range required to represent the elements of the last column of the augmented matrix $\tilde{\mathbf{V}}^{(n)}$ is reduced.

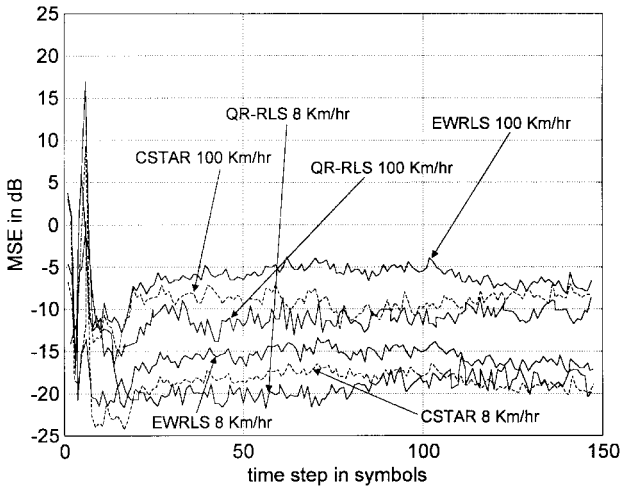

Fig. 2. MSE performance of the adaptive algorithms at different speeds of the mobile and 41.2-μs delay interval in each of the diversity channels.

TABLE I
THE CSTAR TRANSFORMATION

$\mathbf{T}(n)^{(l)}_{k,m}=0\ k,m=1,2,\ldots,L+1$	
if $\left\lvert\frac{\tilde{v}^{(n)}_{L+1,l}\tilde{v}^{(n)*}_{l,l}}{\lvert\tilde{v}^{(n)}_{l,l}\rvert^2}\right\rvert\leq 1\Rightarrow$	(scaling is NOT required) $t=\frac{\tilde{v}^{(n)}_{L+1,l}\tilde{v}^{(n)*}_{l,l}}{\lvert\tilde{v}^{(n)}_{l,l}\rvert^2}$ $\mathbf{T}(n)^{(l)}_{L+1,L+1}=1$ $\mathbf{T}(n)^{(l)}_{l,l}=1$ $\mathbf{T}(n)^{(l)}_{L+1,l}=-t$ $\mathbf{T}(n)^{(l)}_{l,L+1}=t^*$
if $\left\lvert\frac{\tilde{v}^{(n)}_{L+1,l}\tilde{v}^{(n)*}_{l,l}}{\lvert\tilde{v}^{(n)}_{l,l}\rvert^2}\right\rvert>1\Rightarrow$	(scaling is required) $t=csign\{\tilde{v}^{(n)}_{L+1,l}\tilde{v}^{(n)*}_{l,l}\}$, $z=\frac{\tilde{v}^{(n)}_{L+1,l}\tilde{v}^{(n)*}_{l,l}}{\lvert\tilde{v}^{(n)}_{l,l}\rvert^2}t^*$, $t_z=\frac{tz^*}{\lvert z\rvert^2}$, $\overline{z}=\frac{z^*}{\lvert z\rvert^2}$ $\mathbf{T}(n)^{(l)}_{L+1,L+1}=\overline{z}$ $\mathbf{T}(n)^{(l)}_{l,l}=1$ $\mathbf{T}(n)^{(l)}_{L+1,l}=-t$ $\mathbf{T}(n)^{(l)}_{l,L+1}=t_z^*$
$\mathbf{T}(n)^{(l)}_{k,k}=1\ \ k\neq l,L+1$	

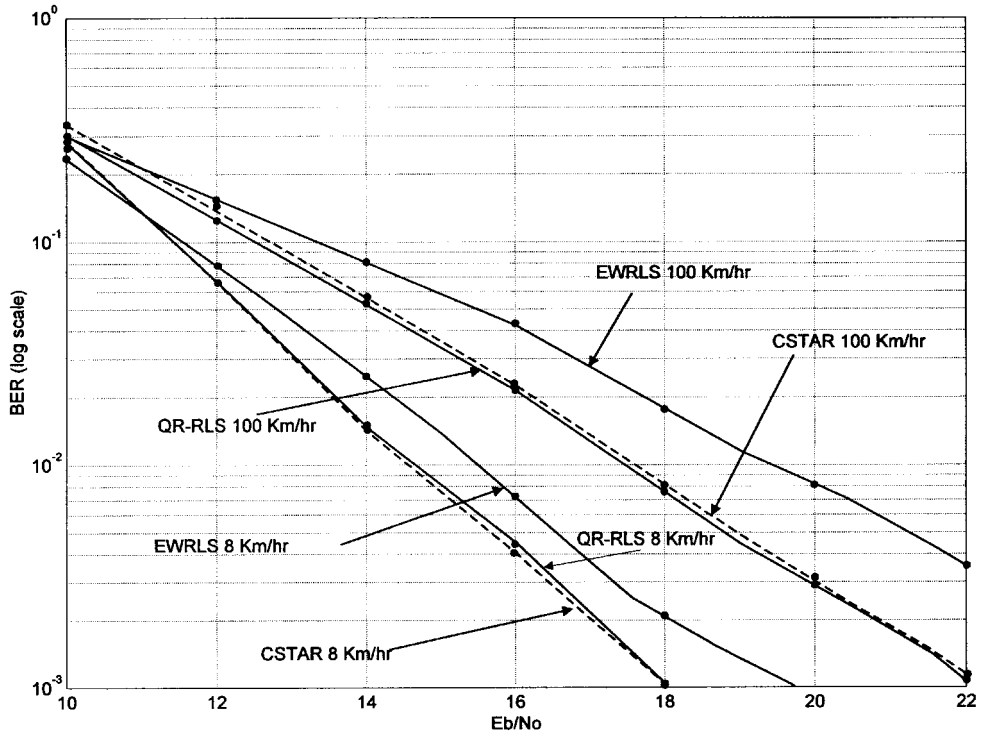

Fig. 3. BER performance of the adaptive algorithms at different speeds of the mobile and 41.2-μs delay interval in each of the diversity channels.

in the flow diagram of the transformation (Table I) that, whenever scaling is required, we obtain a nonorthogonal $\mathbf{T}(n)^{(l)}$ elementary matrix [and of course a nonorthogonal $\mathbf{T}(n)$]. So the CSTAR solution deviates from the optimum least squares solution.[6] However, it is possible to show along the same guidelines of [5] that the deviation from orthogonality is limited to the first few adaption steps because as new samples are processed the scaling operation becomes more and more unnecessary. In other words, the algorithm has the property that

$$\lim_{n\to\infty} \left\| \mathbf{T}(n)^{(l)^H} \mathbf{T}(n)^{(l)} - \mathbf{I} \right\|_F = \mathbf{0}, \quad l = 1, 2, \cdots, L \quad (6)$$

where $\mathbf{I}$ is the identity matrix and we have used the notation $||\mathbf{M}||_F = \sqrt{\sum_{i=1}^{M} \sum_{j=1}^{M} |m_{i,j}|^2}$ for the Frobenius norm of a $M \times M$ complex matrix $\mathbf{M}$ whose generic i, j element is $m_{i,j}$. Our experimental results show that the effect of this initial bias is negligible. The algorithm can be summarized as in Table II. In Table III the computational complexity of the CSTAR method is compared to the QR approach using Givens rotations (defined QRG) and the EWRLS (exponentially windowed RLS of [4]) in terms of real multiplications, reciprocals, square roots, and additions.

[6] In fact at any given step

$$\arg \min_{\partial \mathbf{c}(n)} \left\| \begin{bmatrix} \mathbf{V}_{\mathrm{GR}}^{(n+1)} \\ \mathbf{0^T} \end{bmatrix} \partial \mathbf{c}(n) - \bar{\mathbf{Q}}(n) \begin{bmatrix} 0 \\ u_{n+1} \end{bmatrix} \right\|^2$$
$$\neq \arg \min_{\partial \mathbf{c}(n)} \left\| \begin{bmatrix} \mathbf{V}_{\mathrm{CSTAR}}^{(n+1)} \\ \mathbf{0^T} \end{bmatrix} \partial \mathbf{c}(n) - \mathbf{T}(n) \begin{bmatrix} 0 \\ u_{n+1} \end{bmatrix} \right\|^2$$

where $\mathbf{V}_{\mathrm{GR}}^{(n+1)}$ and $\mathbf{V}_{\mathrm{CSTAR}}^{(n+1)}$ are the triangular matrices obtained from the sweep performed applying Givens rotations and CSTAR rotations, respectively.

TABLE II
THE CSTAR ALGORITHM

Initialization	$\mathbf{c}(n) = \mathbf{0}$, $\mathbf{V}^{(n)} = \gamma \mathbf{I}$
Input	$\mathbf{y}(n+1)$, $\mathbf{c}(n)$, λ, x_n, $\mathbf{V}^{(n)}$
Compute Prediction Error	$u_{n+1} = x_{n+1} - \mathbf{y}(n+1)^T \mathbf{c}(n)$
Form the matrix $\tilde{\mathbf{V}}^{(n)}$	$\tilde{\mathbf{V}}^{(n)} = \begin{bmatrix} \lambda \mathbf{V}^{(n)} & \mathbf{0} \\ \mathbf{y}(n+1)^T & u_{n+1} \end{bmatrix}$
Sweep $\mathbf{y}(n+1)^T$	$\mathbf{T}(n)\ \tilde{\mathbf{V}}^{(n)} \overset{CSTAR}{\Rightarrow} \begin{bmatrix} \mathbf{V}^{(n+1)} & \bar{\mathbf{X}}^{(n+1)} \\ \mathbf{0}^T & r_{n+1} \end{bmatrix}$
Solve by backsubstitution	$\partial \mathbf{c}(n) = \left[\mathbf{V}^{(n+1)}\right]^{-1} \bar{\mathbf{X}}^{(n+1)}$
Obtain new taps	$\mathbf{c}(n+1) = \mathbf{c}(n) + \partial \mathbf{c}(n)$

IV. SIMULATIONS

A TDMA system for cellular communications has been simulated according to [6] and [7]. We assume a two-ray Rayleigh fading diversity channel $(P_1 = P_2 = 2)$ [7]. The delay interval is the difference in time of arrival between the two rays at each antenna. The speed of the transmitter mobile defines the time-varying characteristics of the channel. The frame is constituted by 162 symbols and 14 of them are dedicated to the training sequence. Delay interval for both diversity channels is equal to 41.2 μs (one symbol period) to describe an environment severely affected by intersymbol

TABLE III
COMPUTATIONAL COMPLEXITY PER UPDATE

Method	QRG alg.	EWRLS alg.	CSTAR (no scaling)	CSTAR (scaling)
N. of Real Multiplies	$10L^2+30L$	$6L^2+14L$	$10L^2+32L$	$10L^2+40L$
N. of Reciprocals	$4L$	2	$4L-2$	$4L$
N. of Square Roots	L	0	0	0
N. of Real Additions	$3L^2+3L$	$6L^2-8L+6$	$3L^2+3L$	$3L^2+7L$

interference. The length of the feedforward sections is 3, the length of the feedback section is 2. Sampling rate is $2/T\,(R=2)$. The described algorithm, the EWRLS algorithm (traditional RLS [4]) and the QR-RLS algorithm (traditional QR-based RLS, [3]) have been implemented using 24 bits of resolution in the fixed point arithmetic representation. Fig. 2 shows performance of the CSTAR algorithm compared to EWRLS and to QR-RLS in terms of mean squared error estimated and averaged over 100 runs. The value of λ is 0.855 for 100 km/h and 0.98 for 8 km/h.[7] Fig. 3 shows bit error rate (BER) results. The EWRLS algorithm reveals numerical problems directly impacting BER performance. The CSTAR algorithm achieves performance similar to the traditional Givens-based QR-RLS.

V. CONCLUSIONS

We have presented a new method to update the digital filters of a MMSE 2-antenna space–time decision-feedback receiver. The algorithm is particularly suited for fixed-point arithmetic implementations because it preserves the numerical stability and performance of a QR-based approach but it is less computationally demanding due to the absence of square root operations. Experimental results were presented for the IS-136 North American [6] standard for cellular TDMA communications to validate the method and to confirm the effectiveness of the approach.

[7] In general, low speeds require larger values of λ to get the best performance out of the tracking scheme. However, there is marginal BER degradation if λ is kept fixed to 0.855.

REFERENCES

[1] P. Monsen, "MMSE equalization of interference on fading diversity channels," *IEEE Trans. Commun.*, vol. 34, pp. 5–12, Jan. 1984.
[2] C. Despins, D. Falconer, and S. Mahmoud, "Compound strategies of coding, equalization, and space diversity for wide-band TDMA indoor wireless channels," *IEEE Trans. Veh. Technol.*, vol. 41, pp. 369–379, Nov. 1992.
[3] S. Haykin *Adaptive Filter Theory.* Englewood Cliff, NJ: Prentice Hall, 1986.
[4] J. G. Proakis. *Digital Communications.* New York: McGraw-Hill, 1989.
[5] K. J. Raghunath and K. K. Parhi "Pipelined RLS adaptive filtering using scaled tangent rotations," *IEEE Trans. Signal Processing*, vol. 44, pp. 2591–2604, Oct. 1996.
[6] TIA/EIA/IS-136.1-A, "TDMA cellular/PCS–radio interface–mobile station–base station compatibility–digital control channel," and TIA/EIA/IS-136.2-A, "TDMA cellular/PCS–radio interface–mobile station–base station compatibility–traffic channels and FSK control channel," Oct. 1996.
[7] TIA/EIA/IS-138, "800 MHz TDMA cellular–radio interface–minimum performance standards for base stations," Dec. 1994.